Journal of Organometallic Chemistry, 464 (1994) 47–54

JOM 23813

Concerning the silicon–germanium bond: mass spectral fragmentations of isomeric Si–Ge compounds $R_3EE'R_3$ (E = Si, E' = Ge, R = Ph, Me, $(\eta^5\text{-}C_5H_4)Fe(C_5H_5)$, $(\eta^5\text{-}C_5H_5)Fe(CO)_2$ and $(\eta^5\text{-}C_9H_7)Fe(CO)_2$)

Antonio Guerrero and Jorge Cervantes

Facultad de Quimica, Universidad de Guanajuato, Guanajuato, GTO 36050 (Mexico)

Luis Velasco and Jacobo Gomez-Lara

Instituto de Quimica, Universidad Nacional Autonoma de Mexico, Ciudad Universitaria, Mexico, D.F. (Mexico)

Sneh Sharma, Elvira Delgado and Keith Pannell

Department of Chemistry, University of Texas at El Paso, El Paso, TX 79968-0513 (USA)

(Received January 20, 1993; in revised form April 29, 1993)

Abstract

Isomeric pairs of silicon–germanium compounds containing a Si–Ge bond ($Me_3SiGePh_3$ (I) and $Ph_3SiGeMe_3$ (II); $FpSiMe_2GeMe_3$ (III) and $FpGeMe_2SiMe_3$ (IV) (Fp = $(\eta^5\text{-}C_5H_5)Fe(CO)_2$); $IFpSiMe_2GeMe_3$ (V) and $IFpGeMe_2SiMe_3$ (VI) (IFp = $(\eta^5\text{-}C_9H_7)Fe(CO)_2$); $IFpSiMe_2GePh_3$ (VII) and $IFpGeMe_2SiPh_3$ (VIII)) and the complex $FcSiMe_2GeMe_2Fc$ (IX) (Fc = ferrocenyl) have been synthesized and examined by mass spectrometry.

The $R_3SiGeR'_3$ compounds **I** and **II** exhibit considerable exchange of R groups to produce $[R_{3-n}R'_nSi]^+$ and $[R'_{3-n}R_nGe]^+$ ions in progressively lesser amounts as $n = 1 \rightarrow 2 \rightarrow 3$. For the metal-substituted complexes containing the grouping Fe–Si–Ge fragmentation occurs predominantly via Si–Ge bond cleavage with formation of ions containing the silylene ligand $[Fe{=}SiR_2]^+$. Complexes with the Fe–Ge–Si backbone undergo preferential scission of the Fe–Ge bond, illustrating the general bond strength trend Fe–Si > Si–Ge. Upon direct cleavage of the Si–Ge bond in R_3SiGeR_3 compounds, the percentage of the charge carried by $[R_3Si]^+$ ions significantly exceeds that carried by $[R_3Ge]^+$ ions, reflecting the greater electronegativity of Ge polarizing the Si–Ge bond.

Key words: Silicon; Germanium; Ferrocene; Mass spectrometry

1. Introduction

The first recorded example of a silicon–germanium-bonded compound was in 1934 when Kraus and Nelson [1] reported the synthesis of $Ph_3GeSiEt_3$. Detailed studies of such compounds have been relatively sluggish and it was only in 1986 that the X-ray structural analysis of the Si–Ge bond length was reported [2]. In the past 2 years considerably more attention has been given to such compounds [3], in part because of the use of Si–Ge materials in semiconductors and related devices [4,5], and the surge in interest in polysilanes, polygermanes and polysilylgermanes [6–8].

An early report by Chambers and Glockling [9] reported the mass spectral fragmentation patterns of a series of compounds containing interelement bonds of Group 14. They showed that, in compounds of the type $R_3SiSiR'_3$, ions resulting from the exchange of ligand groups were observed, *e.g.* $[R_2R'Si]^+$ and $[R'_2RSi]^+$. This observation was confirmed by Gaidis *et al.* [10] who suggested the exchange occurred via transient intermediates with bridging R groups, $[R_2Si(\mu\text{-}R)(\mu\text{-}R')SiR'_2]$. Two silicon–germanium compounds, $(PhCH_2)_3GeSiMe_3$ and $Ph_3GeSiEt_3$ were among those reported by Chambers and Glockling. Subsequently Pavlinskii *et al.* [11] studied a series of ethylgermylsilanes and also observed similar 1,2 migrations during fragmentation, while George *et al.* [12] reported ex-

---

Correspondence to: Professor K. Pannell.

0022-328X/94/\$07.00
SSDI 0022-328X(93)23813-D

change between methyl and H ligands in the mass spectral fragmentation of Me_3SiGeH_3.

In our laboratories we possess a range of Si–Ge-bonded compounds with both organic and transition metal organometallic ligands. We are particularly interested in the chemical and structural variations of such inter-Group-14-bonded isomeric compounds, *i.e.* $R_3EE'R'_3$ and $R'_3EE'R_3$. No studies have appeared on the mass spectral fragmentation characteristics of such systems and, since we observed significant effects of metal substitution upon the mass spectral fragmentation patterns of disilanes [13], we investigated, and now report, the related properties of the much rarer Si–Ge systems, *i.e.* $Me_3SiGePh_3$ (**I**) and $Ph_3SiGeMe_3$ (**II**), $FpSiMe_2GeMe_3$ (**III**) and $FpGeMe_2SiMe_3$ (**IV**) ($Fp = (\eta^5\text{-}C_5H_5)Fe(CO)_2$), $IFpSiMe_2GeMe_3$ (**V**) and $IFpGeMe_2SiMe_3$ (**VI**) ($IFp = (\eta^5C_9H_7)Fe(CO)_2$), $IFpSiMe_2GePh_3$ (**VII**) and $IFpGeMe_2SiPh_3$ (**VIII**), and $FcSiMe_2GeMe_2Fc$ (**IX**) (Fc = ferrocenyl).

2. *Experimental details and results*

The various compounds were synthesized using procedures reported in the literature: **I** [1], **II** [2], **III**, **IV**, **V**, **VI**, **VII**, **VIII** [3c] and **IX** [14]. Mass spectra were recorded on a Hewlett–Packard HP 5985B instrument using a 70 eV electron beam for complexes **I**, **II**, **VII**, **VIII** and **IX**, and a 12 eV electron beam for complexes **III**, **IV**, **V** and **VI** in order to observe the parent ions and fragmentation pattern for the latter group. Samples were introduced by direct inlet into the ionization chamber maintained at 125°C. The major ions observed, their relative abundances and the percentages of ion current carried (totalling greater than 85%) are recorded in Tables 1–9. The ion currents reported represent the sum total of the specific fragment described taking into account the envelopes of ions resulting from the isotope distribution. All *m/e* values are based upon the use of ^{74}Ge as the most abundant germanium isotope, but all isotopes are used for the percentage of ion current carried by a particular structural grouping. Computed simulations were performed to produce the data recorded in the Tables, using a simulation technique that was previously reported [13]. A full listing of all ions observed in the spectra are available from the authors.

TABLE 1. Fragmentation scheme of compound $H_{24}C_{21}GeSi$ (I) ($(C_6H_5)_3GeSi(CH_3)_3$ at 70 eV)

	RA (%)	*m/e*	Condensed formula	Fragment	*i* (%)
1	9	378	$H_{24}C_{21}SiGe$	$(C_6H_5)_3GeSi(CH_3)_3^+$	2.4
2	2	363	$H_{21}C_{20}SiGe$	$(C_6H_5)_3GeSi(CH_3)_2^+$	0.5
3	67	305	$H_{15}C_{18}Ge$	$(C_6H_5)_3Ge^+$	13
4	32	301	$H_{19}C_{15}SiGe$	$(C_6H_5)_2GeSi(CH_3)_3^+$	1.1
5	3	259	$H_{15}C_{18}Si$	$(C_6H_5)_3Si^+$	0.3
6	2	243	$H_{13}C_{13}Ge$	$(C_6H_5)_2Ge(CH_3)^+$	0.4
7	100	228	$H_{10}C_{12}Ge$	$(C_6H_5)_2Ge^+$	22
8	77	227	$H_9C_{12}Ge$	$(C_6H_5)Ge(C_6H_4)^+$	12
9	18	197	$H_{13}C_{13}Si$	$(C_6H_5)_2Si(CH_3)^+$	1.7
10	2	181	$H_{11}C_8Ge$	$(C_6H_5)Ge(CH_3)_2^+$	0.4
11	2	166	H_8C_7Ge	$(C_6H_5)GeCH_3)^+$	0.4
12	37	151	H_5C_6Ge	$(C_6H_5)Ge^+$	8.1
14	26	135	$H_{11}C_8Si$	$(C_6H_5)Si(CH_3)_2^+$	2.4
15	3	119	H_9C_3Ge	$Ge(CH_3)_3^+$	0.7
16	7	105	H_5C_6Si	$(C_6H_5)Si^+$	0.6
17	19	77	H_5C_6	$(C_6H_5)^+$	1.6
18	58	73	H_9C_3Si	$(CH_3)_3Si^+$	5.1

3. Discussion

Whereas the fragmentation pattern of disilanes has been extensively investigated and reported [9,11,15], few studies have been reported on silylgermanes [9,11,12]. These studies did not address the properties of isomeric systems. From studies of disilane compounds, several fragmentation pathways are expected including simple cleavage of the Si–Ge bond, cleavage associated with molecular rearrangement and ligand exchange, and cleavage of element 14-alkyl(aryl) ligands. For the metal carbonyl complexes, loss of CO is a fragmentation expected to compete with those described above. All these expected fragmentation routes were observed, with significant variations dependent upon the isomeric nature of the Si–Ge compounds. The isomeric pairs are discussed below, and all per-

TABLE 2. Fragmentation scheme of compound $H_{24}C_{21}SiGe$ (II) ($(C_6H_5)_3SiGe(CH_3)_3$ at 70 eV)

	RA (%)	*m/e*	Condensed formula	Fragment	*i* (%)
1	8	378	$H_{24}C_{21}SiGe$	$(C_6H_5)_3SiGe(CH_3)_3^+$	2.4
2	4	363	$H_{21}C_{20}SiGe$	$(C_6H_5)_3SiGe(CH_3)_2^+$	1.1
3	2	301	$H_{19}C_{15}SiGe$	$(C_6H_5)_2SiGe(CH_3)_3^+$	0.6
4	30	260	$H_{16}C_{18}Si$	$(C_6H_5)_3SiH^+$	2.0
5	49	259	$H_{15}C_{18}Si$	$(C_6H_5)_3Si^+$	5.6
6	5	243	$H_{13}C_{13}Ge$	$(C_6H_5)_2Ge(CH_3)^+$	1.2
7	1	228	$H_{10}C_{12}Ge$	$(C_6H_5)_2Ge^+$	0.3
8	4	224	$H_{14}C_9SiGe$	$(C_6H_5)SiGe(CH_3)_3^+$	0.7
9	1	209	$H_{11}C_8SiGe$	$(C_6H_5)SiGe(CH_3)_2^+$	0.3
10	26	197	$H_{13}C_{13}Si$	$(C_6H_5)_2Si(CH_3)^+$	5.1
11	36	183	$H_{11}C_{12}Si$	$(C_6H_5)_2SiH^+$	9.7
12	14	182	$H_{10}C_{12}Si$	$(C_6H_5)_2Si^+$	1.3
13	45	181	$H_{11}C_8Ge$	$(C_6H_5)Ge(CH_3)_2^+$	5.0
14	12	151	H_5C_6Ge	$(C_6H_5)Ge^+$	1.4
15	11	135	$H_{11}C_8Si$	$(C_6H_5)Si(CH_3)_2^+$	1.1
16	100	119	H_7C_7Si	$(C_6H_5)Si(CH_2)^+$	8.6
16	100	119	H_9C_3Ge	$Ge(CH_3)_3^+$	3.5
17	6	104	H_6C_2Ge	$Ge(CH_3)_2^+$	1.5
18	32	77	H_5C_6	$(C_6H_5)^+$	2.0
19	8	73	H_9C_3Si	$(CH_3)_3Si^+$	0.2

TABLE 3. Fragmentation scheme of compound $H_{20}C_{12}O_2SiGeFe$ (III) ((η^5-C_5H_5)Fe(CO)$_2$Si(CH$_3$)$_2$Ge(CH$_3$)$_3$ at 12 eV)

	RA (%)	m/e	Condensed formula	Fragment	i (%)
1	18	354	$H_{20}C_{12}O_2SiGeFe$	$(\eta^5\text{-}C_5H_5)Fe(CO)_2Si(CH_3)_2Ge(CH_3)_3^+$	16
2	4	339	$H_{17}C_{11}O_2SiGeFe$	$(\eta^5\text{-}C_5H_5)Fe(CO)_2Si(CH_3)_2Ge(CH_3)_2^+$	3.7
3	5	326	$H_{20}C_{11}OSiGeFe$	$(\eta^5\text{-}C_5H_5)Fe(CO)Si(CH_3)_2Ge(CH_3)_3^+$	4.7
4	2	311	$H_{17}C_{10}OSiGeFe$	$(\eta^5\text{-}C_5H_5)Fe(CO)Si(CH_3)_2Ge(CH_3)_2^+$	1.3
5	2	298	$H_{20}C_{10}SiGeFe$	$(\eta^5\text{-}C_5H_5)FeSi(CH_3)_2Ge(CH_3)_3^+$	1.6
6	3	296	$H_{14}C_{10}O_2GeFe$	$(\eta^5\text{-}C_5H_5)Fe(CO)_2Ge(CH_3)_3^+$	1.5
7	3	281	$H_{11}C_9O_2GeFe$	$(\eta^5\text{-}C_5H_5)Fe(CO)_2Ge(CH_3)_2^+$	2.4
8	100	235	$H_{11}C_9O_2SiFe$	$(\eta^5\text{-}C_5H_5)Fe(CO)_2Si(CH_3)_2^+$	34
9	8	207	$H_{11}C_8OSiFe$	$(\eta^5\text{-}C_5H_5)Fe(CO)Si(CH_3)_2^+$	2.6
10	17	177	$H_{15}C_5SiGe$	$Si(CH_3)_2Ge(CH_3)_3^+$	13
11	1	139	H_5C_5Ge	$(\eta^5\text{-}C_5H_5)Ge^+$	0.3
12	4	131	H_5C_2SiGe	$(CH_3)SiGe(CH_2)^+$	3.2
13	1	119	H_9C_3Ge	$Ge(CH_3)_3^+$	0.2
14	3	89	H_3CGe	$Ge(CH_3)^+$	2.0
15	7	73	H_9C_3Si	$Si(CH_3)_3^+$	2.0

centages represent the percentages of total ion current carried by a specific fragment.

3.1. $Me_3SiGePh_3$ (I) (Table 1) and $Ph_3SiGeMe_3$ (II) (Table 2)

Parent ions were observed for both **I** and **II** in similar but low abundance, 2.4% (**I** and **II**). Little fragmentation of these parent ions involved cleavage of methyl or phenyl groups with retention of the Si–Ge bond: **I**, $[Me_2SiGePh_3]^+$ m/e 363 (0.5%), $[Me_3SiGePh_2]^+$ m/e 301 (1.1%); **II**, $[Ph_2SiGeMe_3]^+$ m/e 301 (0.6%), $[Ph_3SiGeMe_2]^+$ m/e 363 (1.1%). The majority of the ions observed in the two spectra were associated with the cleavage of the Si–Ge bond with, and without, ligand exchange. The percentages of total ion current carried by these $[R_3Si]^+$ and $[R_3Ge]^+$ ions are presented in Table 10. It is clear from these data that cleavage of the Si–Ge bond in the parent ion, without ligand exchange, is paramount, but significant exchange occurred prior to total cleavage such that the expected ligand exchanged ions were observed in progressively less abundance as the number of exchange processes required to form the ions increased. This observation is found for both **I** and **II**; there was no equilibration process occurring to render the spectroscopic data for **I** and **II** equivalent. Finally, the data show that in terms of the heterolytic cleavage of the Si–Ge-bonded ions, $[R_3SiGeR'_3]^+$, the major portion of the charge resided on the element containing the phenyl groups, *i.e.* Ge for **I** and Si for **II**.

3.2. $FpSiMe_2GeMe_3$ (III) (Table 3) and $FpGeMe_2SiMe_3$ (IV) (Table 4)

These isomeric complexes exhibited dramatically distinctive fragmentation patterns. Both exhibited parent ions of relatively high abundance (**III**, m/e 16%;

TABLE 4. Fragmentation scheme of compound $H_{20}C_{12}O_2GeSiFe$ (IV) ((η^5-C_5H_5)Fe(CO)$_2$)Ge(CH$_3$)$_2$Si(CH$_3$)$_3$ at 12 eV)

	RA (%)	m/e	Condensed formula	Fragment	i (%)
1	18	354	$H_{20}C_{12}O_2GeSiFe$	$(\eta^5\text{-}C_5H_5)Fe(CO)_2Ge(CH_3)_2Si(CH_3)_3^+$	8.2
2	5	339	$H_{17}C_{11}O_2GeSiFe$	$(\eta^5\text{-}C_5H_5)Fe(CO)_2Ge(CH_3)_2Si(CH_3)_2^+$	2.2
3	2	326	$H_{20}C_{11}OGeSiFe$	$(\eta^5\text{-}C_5H_5)Fe(CO)Ge(CH_3)_2Si(CH_3)_3^+$	1.1
4	3	311	$H_{17}C_{10}OGeSiFe$	$(\eta^5\text{-}C_5H_5)Fe(CO)Ge(CH_3)_2Si(CH_3)_2^+$	1.5
5	2	298	$H_{20}C_{10}GeSiFe$	$(\eta^5\text{-}C_5H_5)FeGe(CH_3)_2Si(CH_3)_3^+$	0.7
6	5	296	$H_{14}C_{10}O_2GeFe$	$(\eta^5\text{-}C_5H_5)Fe(CO)_2Ge(CH_3)_3^+$	1.5
7	8	281	$H_{11}C_9O_2GeFe$	$(\eta^5\text{-}C_5H_5)Fe(CO)_2Ge(CH_3)_2^+$	2.2
8	2	225	$H_{11}C_7GeFe$	$(\eta^5\text{-}C_5H_5)FeGe(CH_3)_2^+$	0.9
9	98	177	$H_{15}C_5GeSi$	$Ge(CH_3)_2Si(CH_3)_3^+$	38
10	4	139	H_5C_5Ge	$(\eta^5\text{-}C_5H_5)Ge^+$	1.7
11	1	121	H_5C_5Fe	$(\eta^5\text{-}C_5H_5)Fe^+$	0.1
12	1	119	H_9C_3Ge	$Ge(CH_3)_3^+$	0.3
13	29	89	H_3CGe	$Ge(CH_3)^+$	11
14	100	73	H_9C_3Si	$Si(CH_3)_3^+$	15

TABLE 5. Fragmentation scheme of compound $H_{22}C_{16}O_2SiGeFe$ (V) ($(\eta^5$-$C_9H_7)(CO)_2FeSi(CH_3)_2Ge(CH_3)_3$ at 12 eV)

	RA (%)	m/e	Condensed formula	Fragment	i (%)
1	31	404	$H_{22}C_{16}O_2SiGeFe$	$(\eta^5\text{-}C_9H_7)(CO)_2FeSi(CH_3)_2Ge(CH_3)_3^+$	9.7
2	8	389	$H_{19}C_{15}O_2SiGeFe$	$(\eta^5\text{-}C_9H_7)(CO)_2FeSi(CH_3)_2Ge(CH_3)_2^+$	2.4
3	36	376	$H_{22}C_{15}OSiGeFe$	$(\eta^5\text{-}C_9H_7)(CO)FeSi(CH_3)_2Ge(CH_3)_3^+$	11
4	3	361	$H_{19}C_{14}OSiGeFe$	$(\eta^5\text{-}C_9H_7)(CO)FeSi(CH_3)_2Ge(CH_3)_2^+$	1.0
5	7	348	$H_{22}C_{14}SiGeFe$	$(\eta^5\text{-}C_9H_7)FeSi(CH_3)_2Ge(CH_3)_3^+$	2.2
6	45	332	$H_{18}C_{13}SiGeFe$	$(\eta^5\text{-}C_9H_7)FeSi(CH_3)_2Ge(CH_3)(CH_2)^+$	24
7	32	331	$H_{13}C_{13}O_2GeFe$	$(\eta^5\text{-}C_9H_7)(CO)_2FeGe(CH_3)_2^+$	6.9
8	42	330	$H_{12}C_{12}OSiGeFe$	$(\eta^5\text{-}C_9H_7)(CO)FeSi(CH_3)Ge(CH_2)^+$	3.3
9	11	316	$H_{10}C_{12}O_2GeFe$	$(\eta^5\text{-}C_9H_7)(CO)_2FeGe(CH_3)^+$	3.2
10	1	303	$H_{13}C_{12}OGeFe$	$(\eta^5\text{-}C_9H_7)(CO)FeGe(CH_3)_2^+$	0.2
11	100	285	$H_{13}C_{13}O_2SiFe$	$(\eta^5\text{-}C_9H_7)(CO)_2FeSi(CH_3)_2^+$	12
12	1	275	$H_{13}C_{11}GeFe$	$(\eta^5\text{-}C_9H_7)FeGe(CH_3)_2^+$	0.2
13	5	260	$H_{10}C_{10}GeFe$	$(\eta^5\text{-}C_9H_7)FeGe(CH_3)^+$	1.5
14	26	257	$H_{13}C_{12}OSiFe$	$(\eta^5\text{-}C_9H_7)(CO)FeSi(CH_3)_2^+$	3.2
15	24	229	$H_{13}C_{11}SiFe$	$(\eta^5\text{-}C_9H_7)FeSi(CH_3)_2^+$	2.8
16	45	177	$H_{15}C_5SiGe$	$(CH_3)_2GeSi(CH_3)_3^+$	12
17	1	119	H_9C_3Ge	$(CH_3)_3Ge^+$	0.4
18	3	89	H_3CGe	$(CH_3)Ge^+$	0.7
19	3	73	H_9C_3Si	$(CH_3)_3Si^+$	0.3

IV, m/e 8.2%) and both exhibited ions associated with the stepwise loss of CO groups occurring in competition with loss of methyl groups. However, a major pathway for fragmentation of III was cleavage of the Si–Ge bond to form a silylene metal ion $[Fp{=}SiMe_2]^+$ (m/e 235 (34%)), a species expected in the light of our previous studies on metal substituted disilanes [13]. Surprisingly, in the case of IV which contains a direct Fe–Ge bond, similar cleavage of the Si–Ge bond to form the analogous ion $[Fp{=}GeMe_2]^+$ was of limited occurrence (m/e 281 (2.2%)). In IV the most abundant ion resulted from direct cleavage of the Fe–Ge bond to form $[Me_3SiGeMe_2]^+$ (m/e 177 (38%)). Such data suggest that the various bond strengths may be ordered as Fe–Si > Si–Ge > Fe–Ge, a result that was verified in the spectra of V, VI, VIII and VIII, *vide infra*. The difference between the fragmentation patterns of III and IV may be observed by viewing the two spectra side by side in Fig. 1 and detailed schematically in general in Scheme 1. It is very obvious that, given the

TABLE 6. Fragmentation scheme of compound $H_{22}C_{16}O_2SiGeFe$ (VI) ($(\eta^5$-$C_9H_7)(CO)_2FeGe(CH_3)_2Si(CH_3)_3$ at 12 eV)

	RA (%)	m/e	Condensed formula	Fragment	i (%)
1	83	404	$H_{22}C_{16}O_2SiGeFe$	$(\eta^5\text{-}C_9H_7)(CO)_2FeGe(CH_3)_2Si(CH_3)_3^+$	19
2	8	389	$H_{19}C_{15}O_2SiGeFe$	$(\eta^5\text{-}C_9H_7)(CO)_2FeGe(CH_3)_2Si(CH_3)_2^+$	1.8
3	75	376	$H_{22}C_{15}OSiGeFe$	$(\eta^5\text{-}C_9H_7)(CO)FeGe(CH_3)_2Si(CH_3)_3^+$	17
4	5	361	$H_{19}C_{14}OSiGeFe$	$(\eta^5\text{-}C_9H_7)(CO)FeGe(CH_3)_2Si(CH_3)_2^+$	1.2
5	14	348	$H_{22}C_{14}SiGeFe$	$(\eta^5\text{-}C_9H_7)FeGe(CH_3)_2Si(CH_3)_3^+$	3.2
6	85	332	$H_{18}C_{13}SiGeFe$	$(\eta^5\text{-}C_9H_7)FeGe(CH_3)_2Si(CH_3)(CH_2)^+$	18
7	54	331	$H_{13}C_{13}O_2GeFe$	$(\eta^5\text{-}C_9H_7)(CO)_2FeGe(CH_3)_2^+$	5.1
8	79	330	$H_{12}C_{12}OSiGeFe$	$(\eta^5\text{-}C_9H_7)(CO)FeGe(CH_3)Si(CH_2)^+$	2.4
9	17	316	$H_{10}C_{12}O_2GeFe$	$(\eta^5\text{-}C_9H_7)(CO)_2FeGe(CH_3)^+$	3.8
10	5	303	$H_{13}C_{12}OGeFe$	$(\eta^5\text{-}C_9H_7)(CO)FeGe(CH_3)_2^+$	1.1
11	1	285	$H_{13}C_{13}O_2SiFe$	$(\eta^5\text{-}C_9H_7)(CO)_2FeSi(CH_3)_2^+$	0.2
12	3	275	$H_{13}C_{11}GeFe$	$(\eta^5\text{-}C_9H_7)FeGe(CH_3)_2^+$	0.7
13	6	260	$H_{10}C_{10}GeFe$	$(\eta^5\text{-}C_9H_7)FeGe(CH_3)^+$	1.3
14	8	244	$H_6C_4O_2SiGeFe$	$(CO)_2FeGe(CH_3)Si(CH_3)^+$	1.6
15	100	177	$H_{15}C_5SiGe$	$(CH_3)_2GeSi(CH_3)_3^+$	20
16	8	89	H_3CGe	$(CH_3)Ge^+$	1.4
17	18	73	H_9C_3Si	$(CH_3)_3Si^+$	1.3

TABLE 7. Fragmentation scheme of compound $H_{28}C_{31}O_2SiGeFe$ (VII) ((η^5-C_9H_7)Fe(CO)$_2$Si(CH$_3$)$_2$Ge(C$_6$H$_5$)$_3$ at 70 eV)

	RA (%)	m/e	Condensed formula	Fragment	i (%)
1	10	534	$H_{28}C_{29}SiGeFe$	$(\eta^5\text{-}C_9H_7)FeSi(CH_3)_2Ge(C_6H_5)_3^+$	2.1
2	12	532	$H_{22}C_{28}OSiGeFe$	$(\eta^5\text{-}C_9H_7)(CO)FeSiGe(C_6H_5)_3^+$	2.4
3	2	476	$H_{22}C_{27}GeFe$	$(\eta^5\text{-}C_9H_7)FeGe(C_6H_5)_3^+$	0.5
4	2	399	$H_{17}C_{21}GeFe$	$(\eta^5\text{-}C_9H_7)FeGe(C_6H_5)_2^+$	0.3
5	2	378	$H_{12}C_{17}O_2GeFe$	$(\eta^5\text{-}C_9H_7)(CO)_2FeGe(C_6H_5)^+$	0.5
6	18	365	$H_{15}C_{16}SiGeFe$	$(\eta^5\text{-}C_9H_7)FeSi(CH_3)Ge(C_6H_5)^+$	0.5
7	62	363	$H_{21}C_{20}SiGe$	$(CH_3)_2SiGe(C_6H_5)_3^+$	11
8	100	306	$H_8C_9O_2SiGeFe$	$(CO)_2FeSi(CH_3)Ge(C_6H_5)^+$	13
8′	100	306	$H_{18}C_{17}SiFe$	$(\eta^5\text{-}C_9H_7)FeSi(CH_3)_2(C_6H_5)^+$	1.8
9	45	305	$H_{15}C_{18}Ge$	$Ge(C_6H_5)_3^+$	3.7
10	58	285	$H_{13}C_{13}O_2SiFe$	$(\eta^5\text{-}C_9H_7)Fe(CO)_2Si(CH_3)_2^+$	4.4
11	12	259	$H_{15}C_{18}Si$	$Si(C_6H_5)_3^+$	0.9
12	15	257	$H_{13}C_{12}OSiFe$	$(\eta^5\text{-}C_9H_7)Fe(CO)Si(CH_3)_2^+$	1.1
13	71	197	$H_{13}C_{13}Si$	$(C_6H_5)_2SiCH_3^+$	4.9
14	13	189	H_7C_9Ge	$(\eta^5\text{-}C_9H_7)Ge^+$	1.0
15	27	171	H_7C_9Fe	$(\eta^5\text{-}C_9H_7)Fe^+$	1.2
16	54	151	H_5C_6Ge	$Ge(C_6H_5)^+$	8.7
17	16	143	H_7C_9Si	$(\eta^5\text{-}C_9H_7)Si^+$	1.0
18	79	135	$H_{11}C_8Si$	$(C_6H_5)Si(CH_3)_2^+$	5.2
19	74	115	H_7C_9	$(C_9H_7)^+$	4.2
20	14	105	H_5C_6Si	$Si(C_6H_5)^+$	0.9

two distinct linkages Fe–Si–Ge and Fe–Ge–Si, mass spectral analysis can immediately distinguish the two isomers by inspection.

3.3. *IFpSiMe$_2$GeMe$_3$ (V) (Table 5) and IFpGeMe$_2$SiMe$_3$ (VI) (Table 6)*

Substituting the η^5-indenyl ligand for the η^5-cyclopentadienyl ligand had little impact upon the mass spectral fragmentation pattern. For **V**, cleavage of the Si–Ge bond occurred to give the most abundant ion as a silylene complex, $[IFp{=}SiMe_2]^+$ (*m/e* 285 (12%)), whereas, for **VI**, cleavage of the Fe–Ge bond occurred most readily to produce $[Me_2GeSiMe_3]^+$ (*m/e* 177 (20%)). Ions equivalent to the germylene complex $[IFp{=}GeMe_3]^+$ were of less abundance than their Si analogs (*m/e* 331 (**V**, 6.9%; **VI**, 5.1%)).

TABLE 8. Fragmentation scheme of compound $H_{28}C_{31}O_2GeSiFe$ (VIII) ((η^5-C_9H_7)Fe(CO)$_2$Ge(CH$_3$)$_2$Si(C$_6$H$_5$)$_3$ at 70 eV)

	RA (%)	m/e	Condensed formula	Fragment	i (%
1	1	590	$H_{28}C_{31}O_2SiGeFe$	$(\eta^5\text{-}C_9H_7)Fe(CO)_2Ge(CH_3)_2Si(C_6H_5)_3^+$	0.3
2	11	534	$H_{28}C_{29}SiGeFe$	$(\eta^5\text{-}C_9H_7)FeGe(CH_3)_2Si(C_6H_5)_3^+$	2.3
3	70	430	$H_{22}C_{27}SiFe$	$(\eta^5\text{-}C_9H_7)FeSi(C_6H_5)_3^+$	6.1
4	17	427	$H_{19}C_{27}SiFe$	$(\eta^5\text{-}C_9H_7)FeSi(C_6H_4)_3^+$	1.5
5	30	368	$H_{10}C_{14}O_2SiGeFe$	$Fe(CO)_2GeSi(C_6H_5)_2^+$	5.9
6	95	363	$H_{21}C_{20}SiGe$	$Ge(CH_3)_2Si(C_6H_5)_3^+$	19
7	4	331	$H_{13}C_{13}O_2FeGe$	$(\eta^5\text{-}C_9H_7)Fe(CO)_2Ge(CH_3)_2^+$	0.7
8	65	259	$H_{15}C_{18}Si$	$Si(C_6H_5)_3^+$	4.9
9	9	257	$H_{13}C_{12}OSiFe$	$(\eta^5\text{-}C_9H_7)Fe(CO)Si(CH_3)_2^+$	0.8
10	80	197	$H_{13}C_{13}Si$	$(CH_3)Si(C_6H_5)_2^+$	5.9
11	29	189	H_7C_9Ge	$(\eta^5\text{-}C_9H_7)Ge^+$	4.7
12	37	171	H_7C_9Fe	$(\eta^5\text{-}C_9H_7)Fe^+$	2.5
13	15	151	H_5C_6Ge	$Ge(C_6H_5)^+$	1.6
14	5	143	H_7C_9Si	$(\eta^5\text{-}C_9H_7)Si^+$	0.4
15	16	135	$H_{11}C_8Si$	$(CH_3)_2Si(C_6H_5)^+$	1.1
16	6	119	H_9C_3Ge	$Ge(CH_3)_3^+$	1.0
17	100	115	H_7C_9	$(C_9H_7)^+$	6.3
18	40	105	H_5C_6Si	$Si(C_6H_5)^+$	2.7
19	12	89	H_3CGe	$Ge(CH_3)^+$	2.0

TABLE 9. Fragmentation scheme of compound $H_{28}C_{31}O_2GeSiFe_2$ (**IX**) ((η^5-C_5H_5)Fe(η^5-$C_5H_4Si(CH_3)_2Ge(CH_3)_2$-$\eta^5$-$C_5H_4$)Fe($\eta^5$-$C_5H_5$) at 70 eV)

	RA (%)	*m/e*	Condensed formula	Fragment	*i* (%)
1	< 1	532	$H_{30}C_{24}SiGeFe_2$	$FcSi(CH_3)_2Ge(CH_3)_2Fc^+$	0.4
2	4.1	289	$H_{15}C_{12}GeFe$	$(\eta^5\text{-}C_5H_5)Fe(\eta^5\text{-}C_5H_4Fe(CH_3)_2)^+$	3.6
3	9.7	259	$H_9C_{10}GeFe$	$(\eta^5\text{-}C_5H_5)Fe(\eta^5\text{-}C_5H_4Ge)^+$	8.4
5	6.5	245	$H_{11}C_{11}SiGe$	$(\eta^5\text{-}C_5H_4)_2GeSi(CH_3)^+$	0.7
6	100	243	$H_{15}C_{12}SiFe$	$(\eta^5\text{-}C_5H_5)Fe(\eta^5\text{-}C_5H_4Si(CH_3)_2)^+$	36
7	2.6	228	$H_{12}C_{11}SiFe$	$(\eta^5\text{-}C_5H_5)Fe(\eta^5\text{-}C_5H_4Si(CH_3))^+$	0.6
8	7.2	213	$H_9C_{10}SiFe$	$(\eta^5\text{-}C_5H_5)Fe(\eta^5\text{-}C_5H_4)Si^+$	2.2
9	10.6	186	$H_{10}C_{10}Fe$	$(\eta^5\text{-}C_5H_5)Fe(\eta^5\text{-}C_5H_5)$	2.9
12	2.2	178	$H_{10}C_7SiFe$	$(\eta^5\text{-}C_5H_4)FeSi(CH_3)_2^+$	0.8
13	5.5	177	H_9C_7SiFe	$(\eta^5\text{-}C_5H_4)FeSi(CH_3)(CH_2)^+$	1.8
14	2.8	169	$H_{11}C_7Ge$	$(C_5H_5)Ge(CH_3)_2^+$	2.2
15	2.5	162	$H_{12}C_4SiGe$	$(CH_3)_2SiGe(CH_3)_2^+$	2.0
16	1.5	147	H_9C_3SiGe	$(CH_3)_2SiGe(CH_3)^+$	0.8
17	4.2	138	H_4C_5Ge	$(\eta^1\text{-}C_5H_4)Ge^+$	3.2
18	21.5	121	H_5C_5Fe	$(\eta^5\text{-}C_5H_5)Fe^+$	6.7
19	2.5	104	H_6C_2Ge	$Ge(CH_3)_2^+$	1.9
20	7.8	93	H_5C_5Si	$(\eta^5\text{-}C_5H_5)Si^+$	2.4

3.4. *IFpSiMe$_2$GePh$_3$ (VII) (Table 7) and IFpGeMe$_2$SiPh$_3$ (VIII) (Table 8)*

The spectra of **VII** and **VIII** were more complex than those of **V** and **VI** owing to the presence of both methyl and phenyl groups on the intra-Group-14 portion of the molecules. This resulted in the type of ligand exchange noted for complexes **I** and **II**. We were able to observe large abundances of the rearranged ions of the type $[Me_2PhSi]^+$ (**VII**, *m/e* 135 (5.2%)) and $[MePh_2Si]^+$ (*m/e* 197 (**VII** 4.9%; **VIII** 5.9%); however, no significant ion abundances were observed for the analogous $[R_3Ge]^+$ species in either spectrum. In the case of **VII** and **VIII**, ion populations were observed for $[IFp{=}SiMe_2]^+$ (*m/e* 285 (4.4%)) and $[IFp{=}GeMe_2]^+$ (*m/e* 331 (0.7%)) respectively. The complexes exhibited major ions for the direct cleavage of the Fe–Ge(Si) bond, *i.e.* $[Me_2Ph_3SiGe]^+$ (*m/e* 363 (**VII** 11%; **VIII** 19%). Finally, with respect to **VIII**, a major germanium free ion at *m/e* = 430 (6.1%) corresponds to $[IFpSiPh_3]^+$, presumably formed by the direct elimination of Me_2Ge from the parent ion. It is noteworthy

TABLE 10. Observed exchange ions

Complex		Ion current (%)		Ion current (%)
I	Me_3Si	5.1	Ph_3Ge	13
	Me_2PhSi	2.4	Ph_2MeGe	0.4
	$MePh_2Si$	1.7	$PhMe_2Ge$	0.4
	Ph_3Si	0.3	Me_3Ge	0.7
II	Ph_3Si	5.6	Me_3Ge	3.5
	Ph_2MeSi	5.1	Me_2PhGe	5.0
	$PhMe_2Si$	1.1	$MePh_2Ge$	1.2
	Me_3Si	0.2	Ph_3Ge	–
III	Me_3Si	2.0	$FpGeMe_2$	2.4
IV	$FpSiMe_2$	–	Me_3Ge	0.3
V	Me_3Si	0.3	$IFpGeMe_2$	6.9
VII	Ph_2MeSi	4.9		
	$PhMe_2Si$	5.2		
	Ph_3Si	0.9		
VIII	Ph_2MeSi	5.9		
	$PhMe_2Si$	1.1		

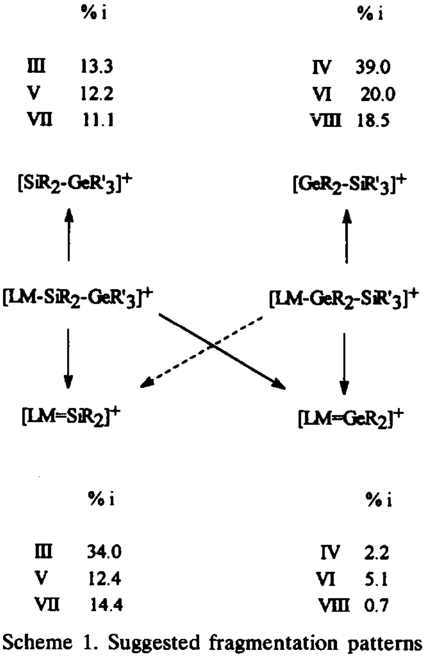

Scheme 1. Suggested fragmentation patterns for **III**, **IV**, **V**, **VI**, **VII** and **VIII**.

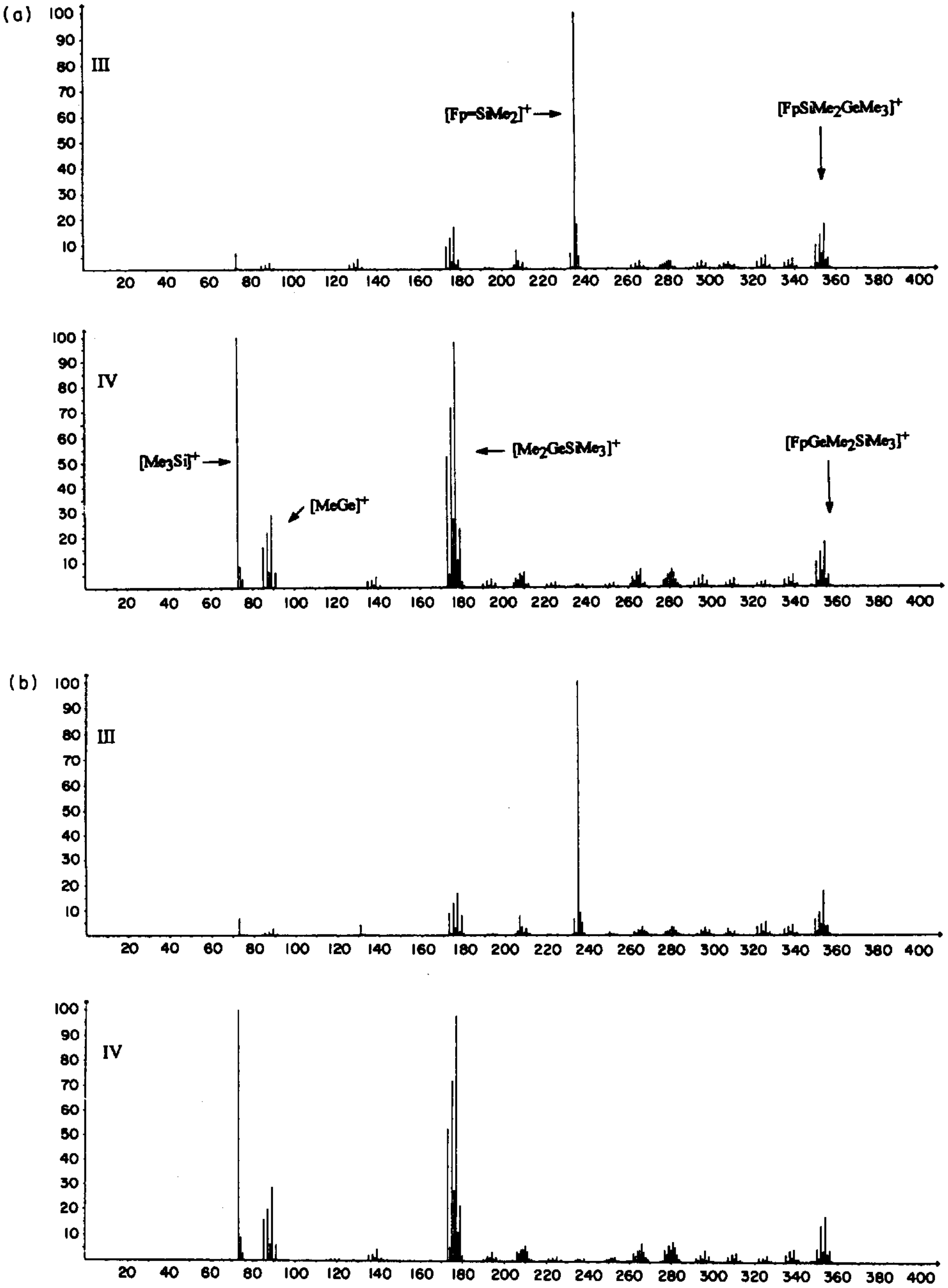

Fig. 1. Simulated (a) and experimental (b) mass spectra for III and IV.

that elimination of $SiMe_2$ from complex VII, containing the Fe–Si–Ge linkage, to form $[IFpGePh_3]^+$ (m/e 476 (0.5%)) was only a minor pathway; the Fe–Si bond is more favoured than the Fe–Ge bond.

4. Conclusions

The following conclusions may be drawn from the data presented and discussed above.

(1) For the non-metal-substituted Si–Ge isomers, significant ligand exchange was observed, and the process continued until total exchange of the R groups attached to both Si and Ge had occurred. The abundances of the ions associated with ligand exchange decreased as the degree of exchange increased (Table 10). This result parallels that reported for two Ge–Sn isomers, $Ph_3GeSnMe_3$ and $Me_3GeSnPh_3$, in which exchange of Ph and Me groups occurred during fragmen-

tation presumably via similar bridging Ph and Me ions [10].

(2) The metal-substituted Si–Ge isomers (LM–Si–Ge, LM–Ge–Si) show distinct differences in behavior. The Fe–Si–Ge complexes exhibited preferential loss of the germyl group via Si–Ge bond cleavage to form silylene type ions, $[LM{=}SiMe_2]^+$ together with a minor amount of Fe–Si cleavage. The Fe–Ge–Si complexes fragment preferentially via Fe–Ge cleavage. This general property is illustrated by the data in Scheme 1. The percentage of total ion current as a function of the two fragmentations, *i.e.* M–Si and Si–Ge or M–Ge and Ge–Si bond cleavage, demonstrates the preference for silylene complex formation over germylene formation, coupled with preferential Fe–Ge cleavage (*cf.* Fe–Si cleavage).

Ligand-exchanged ions, *e.g.* $[FpGeMe_n]^+$ and $[Me_3Si]^+$ from **III**, are observed in relatively minor abundances and are essentially limited to the Fe–Si–Ge systems for the permethylated systems (Table 10). For the Fe–Ge–Si complexes, facile cleavage of the Fe–Ge bond precludes significant formation of the requisite double bridged ions responsible for the exchange process. In the phenyl–methyl complexes **VII** and **VIII**, significant exchange occurs, probably due to the stabilization of the bridging ions by the phenyl group.

(3) For the η^5-cyclopentadienyl and η^5-indenyl (η^5-L) complexes the mass spectra exhibiting ions resulting from the formation of $[\eta^5\text{-LE}]^+$ ions (E = Si, Ge) were observed for both Group 14 elements. Such ring-expanded ions are well established for cyclopentadienyl silicon compounds [12,13].

(4) In general the fragmentation patterns of the Si–Ge compounds illustrate the greater capacity of the Si atom to carry positive charge than the Ge atom. Thus, upon initial cleavage of the Si–Ge bonds in the various compounds studied, the amount of current carried by $[R_3Si]^+$ is greater than that carried by $[R_3Ge]^+$. This is further, and more dramatically, illustrated in the symmetrical complex $FcSiMe_2GeMe_2Fc$ (Table 9). In this case, Si–Ge bond cleavage is the major fragmentation, as was the case for the $FcSiMe_2SiMe_2Fc$ complex [13], and greater than 36% of the charge is carried by $[FcSiMe_2]^+$ (*m/e* 243) compared with 3.6% by the other fragment formed by cleavage of the Si–Ge bond, $[FcGeMe_2]^+$ (*m/e* 289). These results suggest a greater electronegativity of Ge over Si.

Acknowledgments

This research was supported by the National Science Foundation and Consejo Nacional de Ciencia y Tecnologia de Mexico (Grant Int-9002051), the National Science Foundation (Grant RII-88-02973) and the NIH-MARC program (Grant GM 08048).

References

1 C.A. Kraus and W.K. Nelson, *J. Am. Chem. Soc., 56* (1934) 195.
2 L. Parkanyi, C. Hernandez and K.H. Pannell, *J. Organomet. Chem., 301* (1986) 145.
3 (a) K. Mochida, H. Kikkawa and Y. Nakadaira, *Chem. Lett., 7* (1988) 1089; (b) S.P. Mallela and R.A. Geanangel, *Inorg. Chem., 30* (1991) 1480; (c) K.H. Pannell and S. Sharma, *Organometallics, 10* (1991) 1655; (d) K.M. Baines and J.A. Cooke, *Organometallics, 10* (1991) 3419; (e) K.L. Bobbitt and P.P. Gaspar, *Proc. 24th Organosilicon Symp., El Paso, April 12–13, 1991,* Abstract 24; (f) R.S. Grev, H.F. Schaefer III and K.M. Baines, *J. Am. Chem. Soc., 112* (1990) 9458; (g) K. Mochida, H. Kikkawa and H. Nakadaira, *J. Organomet. Chem. 412* (1991) 9.
4 S. Päidassi, *Appl. Phys. Lett., 35* (1979) 886.
5 G. Lucovsky, *J. Non-Cryst. Solids, 76* (1985) 173.
6 R. West, *J. Organomet. Chem., 300* (1986) 327.
7 P. Trefonas and R. West, *J. Polym. Sci., 23* (1985) 2099.
8 (a) N. Matsumoto, K. Takeda, H. Teramae and M. Fujino, *Advances in Silicon Based Polymer Science*, American Chemical Society, Washington, DC, 1989, Chapter 28; (b) K. Takeda, K. Shiraishi and N. Matsumoto, *J. Am. Chem. Soc., 112* (1990) 5043.
9 D.B. Chambers and F. Glockling, *J. Chem. Soc. A* (1968) 735.
10 J.M. Gaidis, P.R. Briggs and T.W. Shannon, *J. Phys. Chem., 75* (1971) 974.
11 V.G. Pavlinskii, V.Yu. Vitkovskii, D.A. Bravo-Zhivotovskii, S.D. Pigarev and N.S. Vyazankin, *Izv. Akad. Nauk SSSR, Ser. Khim., 36* (1987) 1668 (*Bull. Acad. Sci. USSR, Chem. Ser., 36* (1987) 1546).
12 R.D. George, K.M. Mackay and S.R. Stobart, *J. Chem. Soc. A* (1970) 3250.
13 A. Guerrero, J. Gomez-Lara, J. Cervantes, L. Velasco, H. Sharma and K.H. Pannell, *J. Organomet. Chem., 430* (1992) 273.
14 S. Sharma, H. Sharma and K.H. Pannell, manuscript in preparation.
15 (a) J. Tamas, K. Ujszaszy and G. Bujtas, *Magy. Kém. Foly., 76* (1970) 131 (*Chem. Abstr., 73* (1970) 29910q); (b) Y. Nakadaira, Y. Kobayashi and H. Sakurai, *J. Organomet. Chem., 63* (1973) 79; (c) M.E. Childs and W.P. Weber, *J. Organomet. Chem., 86* (1975) 169; (d) J.R. Krause and P. Potzinger, *Int. J. Mass Spectrom. Ion Phys., 18* (1975) 303; (e) F. Höfler, *Monatsh. Chem., 106* (1975) 593; (f) F. Höfler and R. Jannach, *Inorg. Nucl. Chem. Lett., 11* (1975) 743; (g) V.F. Donyagina, V.F. Traven', V.G. Zaikin and B.I. Stepanov, *Izv. Akad. Nauk SSSR, Ser. Khim., 25* (1976) 2117 (*Bull. Acad. Sci. USSR, Chem. Ser., 25* (1976) 1982); (h) Y. Nakadaira, Y. Kobayashi, M. Kira, H. Sakurai, Y. Yamada and Y. Shida, *J. Organomet. Chem., 113* (1976) 249; (i) A.N. Polivanov, A.A. Bernadskii, V.I. Zhun' and V.N. Bochkarev, *Zh. Obsch. Khim., 48* (1978) 2703; (j) L.E. Gusel'nikova, Yu.P. Polyakov and E.N. Buravtseva, *Zh. Obsch. Khim., 59* (1989) 725.